Journal of the Physical Society of Japan
Vol. 73, No. 9, September, 2004, pp. 2539–2542


# Magnetic Structure of $NiCr_2O_4$ Studied by Neutron Scattering and Magnetization Measurements

Keisuke TOMIYASU* and Isao KAGOMIYA[1†]

*Department of Applied Physics, School of Science and Engineering, Waseda University, 3-4-1 Ohkubo, Shinjuku-ku, Tokyo 169-8555*
[1]*Advanced Research Center of Science and Engineering, Waseda University, 3-4-1 Ohkubo, Shinjuku-ku, Tokyo 169-8555*

(Received March 28, 2004)

The magnetic ordering of the normal spinel ferrimagnet $NiCr_2O_4$ below $T_C = 74$ K was reinvestigated by neutron scattering and magnetization measurements on a powder specimen. We found another magnetic transition at $T_S = 31$ K besides $T_C$ in both experiments. The ordering of a ferrimagnetic (longitudinal) component and that of an antiferromagnetic (transverse) component occur at $T_C$ and $T_S$, separately. A new magnetic structure model of $NiCr_2O_4$ below $T_S$ with a spontaneous magnetization of about 0.3 $\mu_B$/formula is proposed based on experimental neutron scattering intensity.

KEYWORDS: $NiCr_2O_4$, chromite, normal spinel, magnetic structure, neutron scattering, magnetization measurements
DOI: 10.1143/JPSJ.73.2539

## 1. Introduction

The ferrimagnets $MnCr_2O_4$, $CoCr_2O_4$ and $NiCr_2O_4$ crystallize into the normal spinel structure; magnetic $Mn^{2+}$, $Co^{2+}$ and $Ni^{2+}$ ions occupy A-sites and magnetic $Cr^{3+}$ ions occupy B-sites. Figure 1 shows the chemical primitive unit cell of a normal spinel structure and the atomic sites in the cell.

The lattices of $MnCr_2O_4$ and $CoCr_2O_4$ are cubic at all temperatures.[8,9] The magnetic moments of $MnCr_2O_4$ and $CoCr_2O_4$ are classified into a ferrimagnetic and a spiral components.[8,9,12] Only the ferrimagnetic component exhibits ordering at $T_C = 43$ K and 97 K, and a transition to a ferrimagnetic spiral structure occurs at $T_S = 18$ K and 25 K, respectively.[8,9,12] The spiral components are described by propagation vectors $(0.60, 0.60, 0)$ and $(0.62, 0.62, 0)$, respectively.[8,9] As an example, the ferrimagnetic spiral structure of $CoCr_2O_4$ below $T_S$ is illustrated in Fig. 2.[9] Note that the B-sites are placed on two sublattices for both the ferrimagnetic and the spiral components.

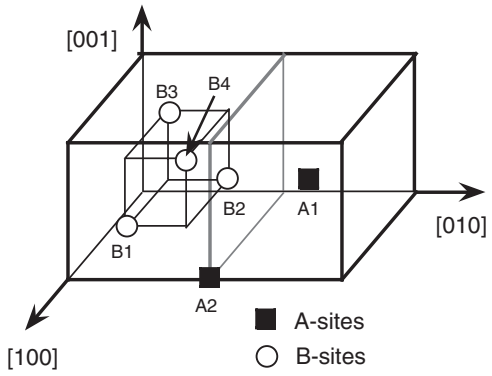


Fig. 1. Sublattices A and B in a chemical primitive unit cell. Atomic sites of oxygen ions are omitted.

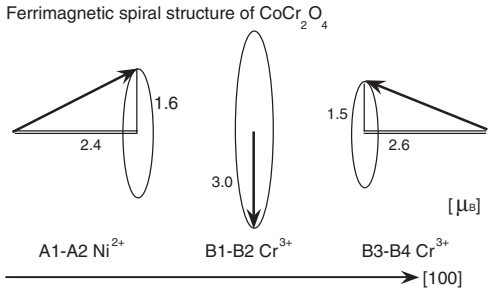


Fig. 2. Ferrimagnetic spiral structure of $CoCr_2O_4$ below $T_S = 25$ K.[9] The spiral component is represented by propagation vector $(0.62, 0.62, 0)$.

On the other hand, the lattice of $NiCr_2O_4$ is elongated tetragonally below 310 K. The value of $(c - a)/a$ is 4% at 4.2 K.[6] The magnetism of $NiCr_2O_4$ reported by Prince,[6] and Bertaut and Dulac[13,14] are summarized as follows. The magnetic moments of $NiCr_2O_4$ are composed of a ferrimagnetic (longitudinal) and an antiferromagnetic (transverse) components, and ordering of the two magnetic components occurs at $T_C = 65$ K simultaneously. The transverse component is represented by propagation vector $Q = (0, 0, 1)$, arising from the large tetragonal distortion. Figure 3 shows the magnetic structure model of $NiCr_2O_4$. The B-sites are regarded as a single sublattice (Nèel model) for the longitudinal component, and are divided into semi-four sublattices for the transverse component.

In fact, the magnetism of $NiCr_2O_4$ should be similar to those of $MnCr_2O_4$ and $CoCr_2O_4$, because all these chromites are similar normal spinel ferrimagnets and are characterized by two magnetic components. However, $NiCr_2O_4$ was reported to exhibit only a single magnetic transition at $T_C$, and the way to assort the B-sites in the magnetic structure model also differs from that in $MnCr_2O_4$ and $CoCr_2O_4$. In particular, the magnetic structure model of $NiCr_2O_4$ involves a major defect which is that the magnitude of spontaneous magnetization is 1.2 $\mu_B$/formula, which is too large compared to that of about 0.3 $\mu_B$/formula estimated by magnet-

*E-mail: k-tommy@aoni.waseda.jp
†Present address: National Institute of Advanced Industrial Science and Technology, Tsukuba, Ibaraki 305-8568.

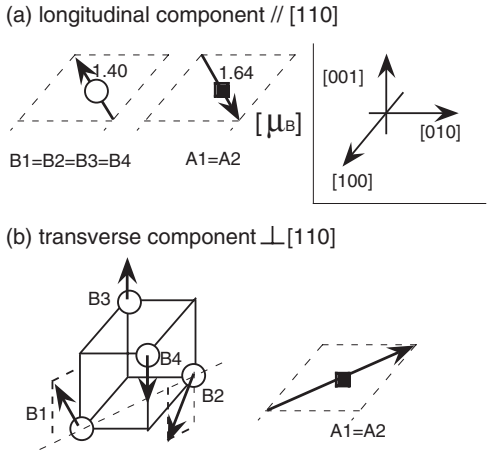


Fig. 3. Previous magnetic structure model of $NiCr_2O_4$ below $T_C$ proposed by Bertaut and Durac.[13,14] The ordering of the ferrimagnetic (longitudinal) component is described by the Nèel model. The ordering of the antiferromagnetic (transverse) component is represented by propagation vector $Q = (0, 0, 1)$.

ization measurements.[3]

Klemme *et al.* recently found an unknown transition at 29 K by heat-capacity measurements, and presumed the ordering of the longitudinal component and that of the transverse component to occur at $T_C$ and $T_S$, separately.[18] The present paper confirms Klemme *et al.*'s speculation by magnetization and neutron scattering measurements. In addition, based on experimental neutron magnetic scattering intensity, we propose a new magnetic structure model of $NiCr_2O_4$ with the spontaneous magnetization of about $0.3\,\mu_B$/formula, in which the B-sites are grouped into two sublattices for both the longitudinal and the transverse components like in $MnCr_2O_4$ and $CoCr_2O_4$.

## 2. Experiments

A powder specimen of $NiCr_2O_4$ was synthesized from a stoichiometric mixture of NiO and $Cr_2O_3$ at 1200°C in air. The sample used for Prince's neutron powder diffraction experiments was also prepared by the same method.[6] Figure 4 shows an X-ray powder diffraction pattern of the present sample at room temperature. No extra lines, which cannot be explained by the spinel structure, are observed.

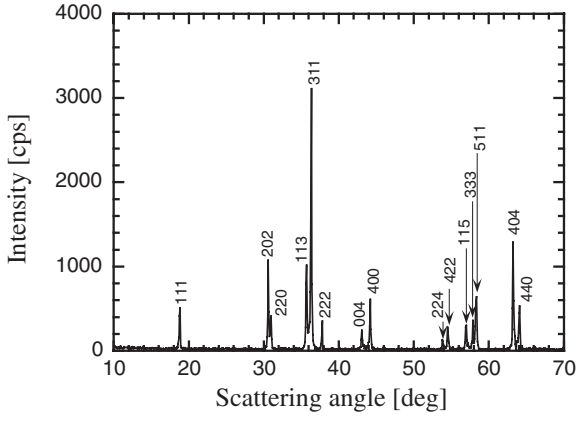


Fig. 4. X-ray powder diffraction pattern at room temperature. Several peaks split into two owing to the tetragonal lattice elongation.

Magnetization measurements were performed in a superconducting quantum interference device (SQUID) system at the Materials Characterization Central Laboratory, Waseda University, Japan. Neutron scattering experiments were performed on the T1-1 triple axis spectrometer installed at a thermal guide of JRR-3M, Tokai, Japan. The energy of the incident neutrons was fixed at 13.5 meV. A pyrolytic graphite filter efficiently eliminated higher-order contamination. The sample was enclosed in a cylindrical vanadium folder with a diameter of 10 mm with $^4$He exchange gas, which was mounted on the cold head of a closed-cycle He refrigerator.

## 3. Results

Figure 5(a) shows the temperature dependence of magnetization studied under field cooling condition. A magnetic field of 100 Oe was applied. In addition to the Curie temperature $T_C = 74$ K, another anomaly was observed at $T_S = 31$ K. The anomaly is most likely identical to the transition at 29 K reported by recent heat-capacity measurements.[18] Figure 5(b) shows the hysteresis loop of magnetization studied at 5 K. Spontaneous magnetization of the present sample is also estimated to be about $0.3\,\mu_B$/formula by linearly extrapolating the high field magnetization to zero field.

Figure 6 shows the neutron powder diffraction patterns at 100 K, 50 K and 15 K. The fundamental reflections and the $Q = (0, 0, 1)$ superlattice reflections are observed at 15 K. The former and latter reflections come from the ferrimagnetic and antiferromagnetic components, respectively.

The neutron scattering line profiles of the 111 fundamental reflection and the 110 superlattice reflection at 100 K,

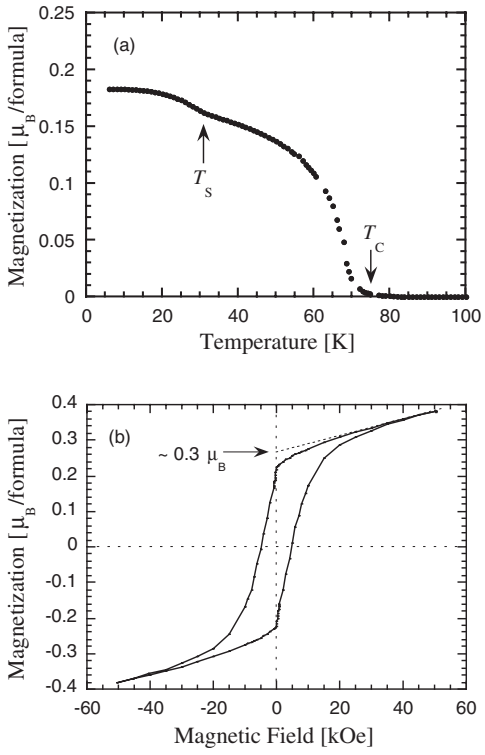


Fig. 5. (a) Temperature dependence of magnetization measured after field cooling. A magnetic field of 100 Oe was applied. (b) Hysteresis loop at 5 K.

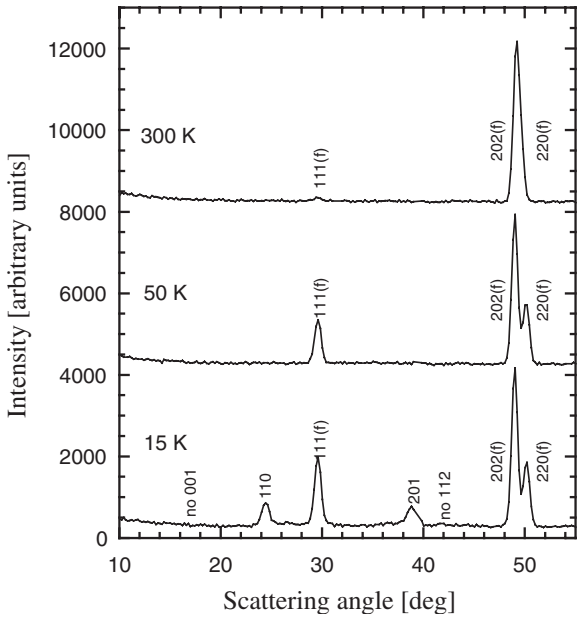


Fig. 6. Neutron powder diffraction patterns at 100 K, 50 K and 15 K. The symbol (f) means fundamental reflection.

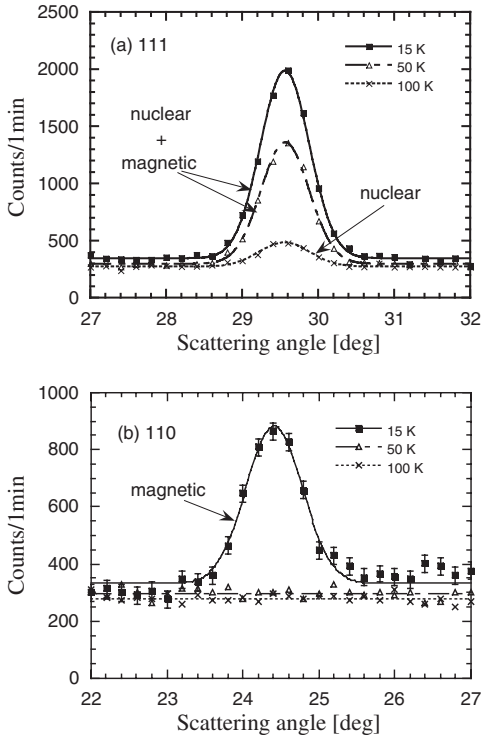


Fig. 7. Neutron scattering line profiles of the 111 fundamental and the 110 superlattice reflections at 100 K, 50 K and 15 K.

50 K and 15 K are magnified in Figs. 7(a) and 7(b), respectively. As the temperature decreases, the magnetic component of the 111 fundamental reflection appears at 50 K, while the 110 superlattice reflection is not observed at 50 K within statistical uncertainty. The 111 fundamental reflection at 100 K is due to nuclear scattering. Therefore, only the order of the longitudinal component of magnetic moments occurs at 50 K.

Figure 8 shows the temperature dependence of the peak intensity of these reflections. We can neglect uncertainty coming from the shift of the peak position accompanied by the thermal contraction of the lattice from 100 K to 15 K, because the shift is within the instrumental resolution in this temperature range. As the temperature decreases, only the longitudinal component appears at $T_C = 74$ K, and the transverse component emerges at $T_S' = 35$ K.

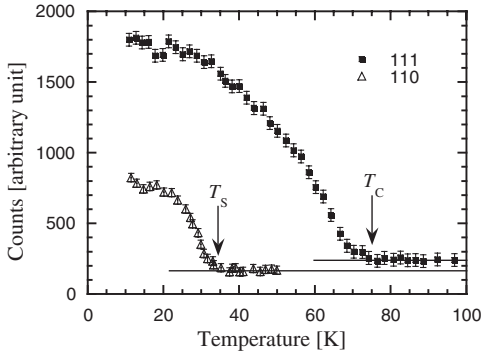


Fig. 8. Temperature dependence of the peak intensity of the 111 fundamental and the 110 superlattice reflections.

The value of $T_S'$ is a little higher than that of $T_S$. This fact can be explained by the difference between time scale in neutron scattering and that in magnetization measurements. Since dynamical spin correlation is observed through the resolution window in neutron scattering, only the component fluctuating slower than the energy-resolution limit is observed. The present resolution was of the order of $10^{11}$ Hz. In contrast, the time scale in magnetization measurements is of the order of $10^{-1}$ Hz, because the response is observed in a uniform and static magnetic field. Therefore, the discrepancy between $T_S'$ and $T_S$ means that the transverse component fluctuates dynamically retaining the correlation at $T_S'$ and its static ordering occurs at $T_S$ with decreasing temperature. This phenomenon is not a surprise because very weak but finite diffuse magnetic scattering, which is the sign of dynamical correlation, persists even at liquid nitrogen temperature 77 K far above $T_S$ determined by magnetization measurements in $MnCr_2O_4$ and $CoCr_2O_4$.[8,9]

It should also be mentioned that both the longitudinal component below $T_C$ and the transverse component below $T_S'$ exhibit long-range order. Since the fundamental and the superlattice reflection lines are as sharp as the instrumental resolution, the correlation length is estimated to be longer than the instrumental resolution limit of 20 nm.

Table I gives the experimental integrated intensity of magnetic scattering. The experimental magnetic scattering integrated intensity of the fundamental reflections was obtained by subtracting the data at 100 K from those at 15 K, and that of the superlattice reflections was obtained by subtracting the data at 50 K from those at 15 K. To determine the magnetic structure of $NiCr_2O_4$ at 15 K ($T < T_S$), these intensities at 15 K were calculated so as to best fit the observed values by varying the ratio of the magnitude of the transverse component to that of the longitudinal component and the direction of each component in a least squares method. In the calculations, we assumed both the longitudinal and the transverse components to be collinear (only up and down) structures, and fixed the magnitudes of the total

Table I. Experimental and best-fit calculated magnetic scattering intensity. The multiplicity of the tetragonal domains is also given. The symbol N.O. means that no reflection was observed within statistical uncertainty.

| *hkl* | Multiplicity | Experimental | Calculated |
|---|---|---|---|
| 001 | 2 | N.O. (< 70) | 0 |
| 110 | 4 | 499 | 533 |
| 201 | 8 | 429 | 423 |
| 112 | 8 | N.O. (< 80) | 100 |
| 002 + 200 | 2 + 4 | N.O. (< 80) | 0 |
| 111 | 8 | 1430 | 1426 |
| 220 + 202 | 4 + 8 | N.O. (< 150) | 149 |
| *R*-factor | — | — | 1.0% |

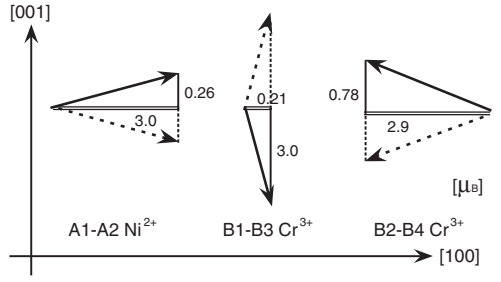


Fig. 9. The new magnetic structure model of $NiCr_2O_4$ below $T_S = 31$ K. The transverse component exhibits collinear (only up or down) antiferromagnetic ordering described by propagation vector $Q = (0, 0, 1)$.

magnetic moments of the $Ni^{2+}$ and $Cr^{3+}$ ions at their theoretical values of $3\,\mu_B$.[16] For the magnetic form factors of the $Ni^{2+}$ and $Cr^{3+}$ ions, the values reported by Watson and Freeman were used.[4] The multiplicity of the tetragonal domains for each scattering and the best-fit calculated intensity are given in Table I.

Figure 9 shows the new magnetic structure model. This new magnetic structure possesses a spontaneous magnetization of $0.3\,\mu_B$/formula, which is consistent with the magnetization measurements. The summation of the longitudinal component of the magnetic moments at the A-sites is larger than that at the B-sites, which is compatible with other magnetization measurements.[16] The longitudinal component (the spontaneous magnetization) is perpendicular to the *c*-axis, agreeing with a Mössbauer spectroscopy study of $^{61}Ni$.[15]

## 4. Discussion

The new magnetic structure model of $NiCr_2O_4$ is characterized by the fact that the four B sublattices are classified into the B1–B3 and B2–B4 pairs for the spontaneous magnetization along the [100] direction (or the B1–B4 and B2–B3 pairs for the spontaneous magnetization along the [010] direction). The ferrimagnetic spiral ordering of cubic $MnCr_2O_4$ and $CoCr_2O_4$ is described by the B1–B2 and B3–B4 pairs, as shown in Fig. 2. Furthermore, the Yafet–Kittel triangular magnetic configuration in the normal spinel system $CuCr_2O_4$, whose lattice is contracted with a tetragonal distortion of 9% at 4.2 K, is also expressed by the B1–B2 and B3–B4 pairs.[2] Thus, we consider that such combinations with respect to the B sublattices is due to the tetragonal lattice elongation (not contraction) of $NiCr_2O_4$ in the 3*d*-metal chromite normal spinel systems $MCr_2O_4$ ($M$ = Mn, Fe, Co, Ni, Cu).

The magnetic ordering of $FeCr_2O_4$ is also described by two magnetic components, the ferrimagnetic one and the spiral one.[10,11] The more precise magnetic structure has not been determined yet.[10,11] However, since the lattice in $FeCr_2O_4$ is contracted with a tetragonal distortion of 3% at 4.2 K,[11] the four B sublattices are expected to be grouped into the B1–B2 and B3–B4 pairs, as for $MnCr_2O_4$, $CoCr_2O_4$ and $CuCr_2O_4$. We intend to reinvestigate the magnetic ordering of $FeCr_2O_4$ in the future.

The KDLM theory and the LKDM theory predicted some magnetic structures by solving the Heisenberg Hamiltonian for the 3*d*-metal $MCr_2O_4$.[5,7] However, a structure with the unique B-sublattice pairs obtained in the present magnetic structure of $NiCr_2O_4$ was not proposed.[5,7] The reason may be that a plausible magnetic structure of $NiCr_2O_4$ was not determined at that time. More detailed theory is required to explain the magnetic structures of the 3*d*-metal $MCr_2O_4$ systematically.

Anderson proposed the concept of magnetic geometrical frustration coming from the tetrahedron (pyrochlore lattice) composed by the B-sites for the cubic normal spinel systems.[1] The antiferromagnetic short-range correlation, which is the sign of magnetic geometrical frustration, was actually observed in other 3*d*-metal chromite $ZnCr_2O_4$.[17] However, the magnetic ordering of $NiCr_2O_4$ exhibits long-range order below $T_S$. The reason is most likely the large tetragonal distortion of $NiCr_2O_4$. This distortion removes the condition that all B–B distances and B–O–B angles are the same, and completely suppresses the magnetic geometrical frustration, as discussed in the case of $CuCr_2O_4$ by Prince.[2]

## Acknowledgment

We thank Professor K. Kohn, Professor K. Siratori, Professor Y. Tsunoda and Dr. K. Kamazawa for their fruitful advice and discussion. We also thank Mr. H. Suzuki for his support in the experiments. This work was supported by Waseda University Grand for Special Research Projects (No. 2003A-589).

1) P. W. Anderson: Phys. Rev. **102** (1956) 1008.
2) E. Prince: Acta Crystallogr. **10** (1957) 554.
3) I. S. Jacobs: J. Phys. Chem. Solids **15** (1960) 54.
4) R. E. Watson and A. J. Freeman: Phys. Rev. **120** (1960) 1134.
5) T. A. Kaplan, K. Dwight, D. H. Lyons and N. Menyuk: J. Appl. Phys. **32** (1961) 13S.
6) E. Prince: J. Appl. Phys. **32** (1961) 68S.
7) D. H. Lyons, T. A. Kaplan, K. Dwight and N. Menyuk: Phys. Rev. **126** (1961) 540.
8) J. M. Hastings and L. M. Corliss: Phys. Rev. **126** (1962) 556.
9) N. Menyuk, K. Dwight and A. Wold: J. Phys. (Paris) **25** (1964) 528.
10) G. L. Bacchella and M. Pinot: J. Phys. (Paris) **25** (1964) 537.
11) G. Shirane and D. E. Cox: J. Appl. Phys. **35** (1964) 954.
12) R. Plumier: J. Appl. Phys. **39** (1968) 635.
13) E. F. Bertaut and J. Dulac: Acta Crystallogr., Sect. A **28** (1972) 580.
14) E. F. Bertaut and J. Dulac: Acta Crystallogr., Sect. A **36** (1980) 157.
15) J. Nakamura *et al.*: RIKEN Rev. **16** (1997) 25.
16) A. N. Goryaga, L. G. Antoshina, A. I. Kokorev and D. A. Chursin: Phys. Solid State **44** (2002) 663.
17) S.-H. Lee *et al.*: Nature (London) **418** (2002) 856.
18) S. Klemme and J. C. Miltenburg: Phys. Chem. Miner. **29** (2002) 663.